Spat. Inf. Res. (2020) 28(6):669–681
https://doi.org/10.1007/s41324-020-00325-x

Synergistic use of Sentinel-1 and Sentinel-2 for improved LULC mapping with special reference to bad land class: a case study for Yamuna River floodplain, India

Armugha Khan[1] · Himanshu Govil[2] · Gaurav Kumar[1] · Rucha Dave[1]

Received: 7 December 2019 / Revised: 27 February 2020 / Accepted: 29 February 2020 / Published online: 11 March 2020

Abstract High accuracy land use/land cover (LULC) mapping of Yamuna Chambal ravines for reclamation and conservation of these degraded/badlands is indispensable. Integration of freely available SAR datasets along with medium to high resolution optical data is one of the best approach for high accuracy LULC mapping. The objective of the presented study is to evaluate the fusion technique for Sentinel-1 SAR data and Sentinel-2 optical data for high accuracy LULC mapping in order to assess the area occupied by these negative landforms i.e., ravines. The VH-polarization fused image with Sentinel-2 optical data gives the best accuracy of 85% followed by VV-polarization fused image with same datasets of 84% accuracy whereas Sentinel-1 and Sentinel-2 provides the accuracy of 60 and 80%, respectively. The prepared LULC maps shown that bad land (Ravine class) occupied an area in the range of 600–700 km^2 using combinations of different datasets as the wastelands in the area required immediate reclamation and conservation measures to be adopted. However, asymptotic performance of fusion technique for SAR and optical data further elucidate its successful implementation and dominancy over other datasets for improved LULC mapping.

Keywords Fusion · Badlands · Land use/land cover · Reclamation · Conservation

✉ Armugha Khan
armrahi4314@gmail.com

Himanshu Govil
himgeo@gmail.com

Gaurav Kumar
gaurav.200490@gmail.com

Rucha Dave
rch.dave1@gmail.com

[1] Department of Basic Sciences, Anand Agricultural University, Anand, Gujarat, India

[2] Department of Applied Geology, National Institute of Technology, Raipur, Chhattisgarh, India

1 Introduction

Increasing rate of anthropogenic activities on the earth's surface and conspicuously in alluvial river flood plains has very wide negative environmental effects. Yamuna river flood plain in and around the Agra district witness an aggravated rate of urbanization. Land degradation and declining agricultural practices around Yamuna–Chambal river valley are another great concerns for land use–land cover (LULC) planning [1, 2]. Formation of gullies and badlands leads ultimately to the mass movement or removal of the productive layers of the surface. These natural hazards (formation of bad lands) are also associated with vicarious climate, low soil moisture, extreme variation in temperature and heavy biotic pressure and reported as the single most wide spread hazard on the earth's surface [3, 4]. However, a declining trend in ravine development was reported [5] but increasing trend of urbanization is another major issue in these fertile Yamuna–Chambal region. Extent monitoring of these wasteland using space technology was initiated by Bali et al. [6] using aerial photography and remote sensing images. To monitor these over exploited degraded lands with medium to high resolution satellite remote sensing and field observations is supposed to be an essential practice for the twenty-first century [7]. LULC mapping and geomorphic feature identification are intrinsic parameters for sound environmental understanding in order to manage the water and

land resources [8, 9]. Therefore, high accuracy mapping of these waste land and other LULC classes around this natural flood plain area using latest available SAR and optical datasets is inevitable.

The contribution of remote sensing in conventional mapping methods is indispensable which makes LULC mapping a reasonable practice. Optical remote sensing data has long back date history of its contribution in LULC mapping. In particular, Landsat series data has been widely used for the same purpose and about 100,000 studies using it has been carried out since 2008 due to its free availability [10]. In the study area, LULC mapping using Landsat-8 has been carried out by Khan et al. [11] and Ali et al. [12] but the results in the study appears noteworthy while applying Sentinel-2 (medium resolution sensors) datasets for LULC mapping purposes. As reported previously that Sentinel-2 is the follow up mission of Landsat series and intended to provide continuity of data with some sort of consistent advancements [13]. The application of Sentinel-2 data has also gain huge acceptance due to its high spatial resolution and improved spectral resolution in Near Infra-Red region providing wide applicability for classification, mapping and monitoring purposes [14]. Further, SAR imaging has different imaging principles as compared to optical remote sensing and its image appearance depends on the geometry, roughness, content of the material and the wavelength of the SAR from the target [15]. SAR data is complementary to the optical data because of its physical observation of the target in terms of different scatterings [16]. Therefore, Sentinel-1 SAR data in LULC mapping particularly for its all-weather functional capability and sensitivity towards natural targets has been significantly inferred for LULC mapping [17]. Different studies entails LULC mapping based objectives involving the use of Sentinel-1 radar data have been reported from different environment including Indian monsoon regions [9]. Sentinel series occupies a huge space in earth observations particularly due to high operational ability, long term continuity, superior calibration of sensors and a variety of sensing methods and products for the scientific community [18]. Free availability of majority of sentinel products further makes it dominating datasets for earth monitoring studies.

Integration of images acquired on different part of electro-magnetic spectrum provides complementary information, therefore, found useful for discrimination of different LULC classes and consequently improves the accuracy of classified maps. Different type of fusion techniques are used for different objectives but in case of LULC mapping preparation of high accuracy maps is the foremost task. Recently, a study differentiating grassland from Alfalfa biofuel in Canada and a similar study to distinguish dwellers in refugee camps using fusion of optical and SAR datasets were successfully carried out by Amarsaikhana et al. [16] and Sprohnle et al. [19]. Fusion of different band (X, C and L band) SAR datasets including Terra SAR X, Radarsat-1, Radarsat-2 and ALOS PALSAR with optical Landsat, SPOT and MODIS data were carried out by several authors for improved LULC classifications [20, 21]. The studies on different classification algorithms including neural network (NN), support vector machine (SVM), random forest (RF) and maximum likelihood (MLC) etc. on fused datasets (using different methods) are carried out on large scale but extraction of information using these datasets on fine resolution is still debatable.

Numerous ways of integration of SAR and optical data are in use but fusion techniques has consistently been reported as the most robust technique. In general, number of fusion techniques have been developed in order to improve the accuracy of the output image including pixel level fusion, feature level fusion and decision level fusion. Wavelet based transformation, Brovey transformation, Ehlers and principal component analysis are the commonly used pixel level fusion methods. Fusion technique involves spatial characters of a panchromatic image combined with spectral structure of low resolution of multispectral image in order to improve spatial, temporal and spectral resolution, prior to the classification [22]. The fusion of SAR and optical data has enormous applications in natural resource monitoring. Landslide detection, erosional landform mapping susceptible to mass movement and crop mapping in agricultural sciences are some of the crucial themes required up to date land use land cover maps of the study sites. Fusion causes the debility in the colour and ultimately the quality of the image but the main objective of the fusion technique is to enhance the attributes of a particular feature to reduce confusion. Though, Ehlers [23] proposed a new method by eliminating these effects to produce a much higher quality image using filtering in the Fourier domain [22]. Ehler's fusion is a pixel level, intensity–hue–saturation (HIS) transformation based fusion technique, adopted in the present study. The technique has successfully implemented and having its dominancy on the other existing fusion techniques [24].

Moreover, a LULC comparison between the fused datasets of Sentinel-1 and 2 with separate Sentinel-1 and Sentinel-2 data is presented in this paper. Mapping of Yamuna–Chambal ravine on large scale using optical dataset alone was carried out by several workers but no study using SAR datasets for such waste land features, extent and the other LULC classes mapping on Yamuna river flood plain has so far been carried out. However, accurate information about extent and nature of these wastelands is essential for adaptation of suitable reclamation policy in parts of Yamuna river flood plain, therefore, these high accuracy LULC map becomes indispensable for the sustainable development of the region. The study aimed

to compare the performance of SAR, Optical and fused images of SAR and optical data for LULC classification purpose with special reference to wasteland class in parts of Yamuna River flood plain.

2 Study area

The lower Yamuna River basin around Agra district is considered as the study area after perceiving higher rate of human intervention and land degradation. The boundary of the study area was demarcated on the basis of the watershed analysis in this particular part of Yamuna River flood plain (Fig. 1). Geographically, 26°30′ to 27°15′ N latitude and 78°0′ to 79°15′ E longitude bounded the region under present investigation. Agra, Firozabad and Etawah districts lies in the lower Yamuna Basin falls in the study area covering almost 2915 km^2 area. The selection of area in and around the main channel of Yamuna River deceits in the fact that this is the most degraded flood plain of the river due to anthropogenic activities. Increasing rate of urbanization and exploitation of surface and ground water are consistently deteriorating the existed landscape. Besides, the presence of badlands formed due to accelerated rate of gully, sheet, rill and ravenous erosion is the major environmental threat in the study area [11]. Around 1.23 million hectare of land is under ravines along the bank of Yamuna River in this region [4]. In addition, the average rainfall in the study area ranges in between 700 and 900 mm and the climate of the region is arid. However, in accordance with the [25] study area falls in the warm temperate, steppe with hot summer climate category. Geologically, the study area is covered by newer alluvium along the channel followed by older alluvium covered the entire flood plain of the study area. Some outcrops of Vindhyan sandstone encountered in the south western portion of the area which are believed to be the basement rock in the region.

3 Data and methods

Presented study is carried out using both Sentinel datasets including C-band Sentinel-1 SAR and Sentinel-2 multispectral data launched on 2014 and 2015, respectively. The datasets acquisition period along with the sources and other characteristics have been tabulated in Table 1. The processing is carried out using Sentinel Application Platform (SNAP) for Sentinel-1 SAR whereas Sentinel-2 data was pre-processed to carry out the atmospheric correction. The maximum likelihood approach (MLC) algorithm was adopted to perform supervise classification of the given datasets. The pre-processing steps followed in the present study are discussed in detail and the methodology flow chart is given below (Fig. 2).

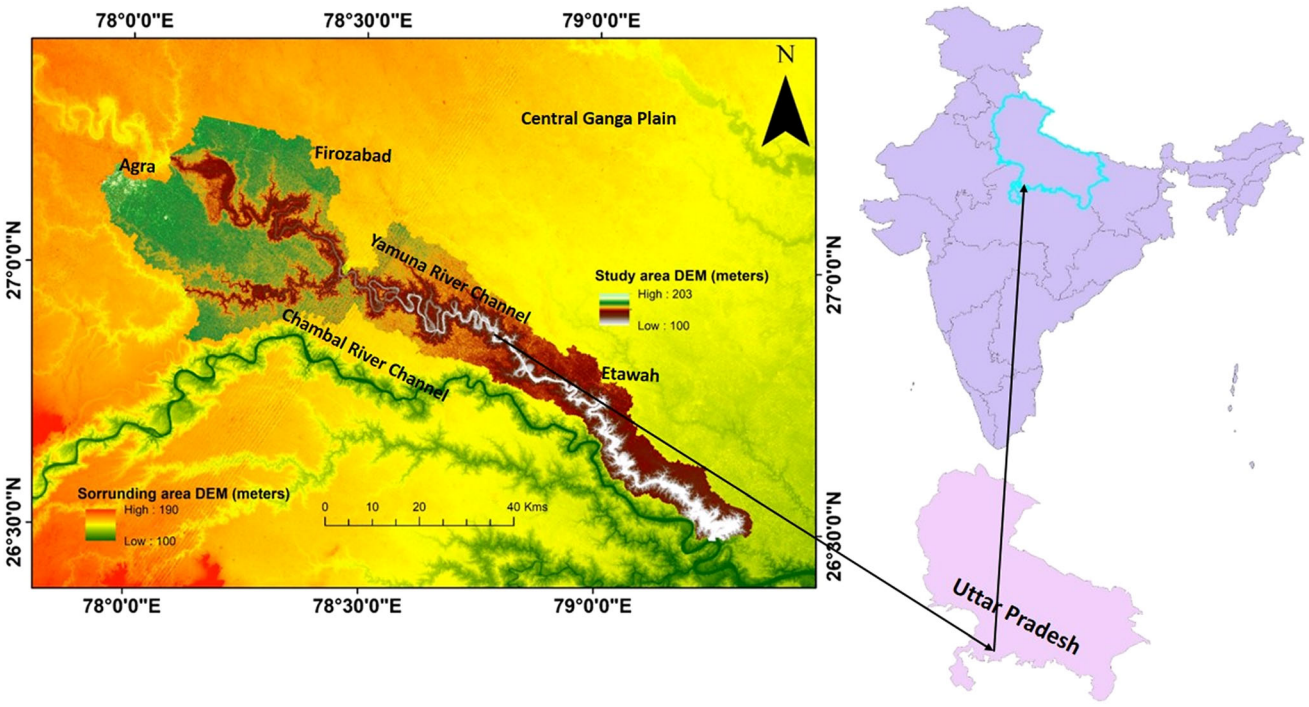

Fig. 1 Map of the Yamuna River flood plain study area around Agra, Firozabad and Etawah district, Uttar Pradesh, India

Table 1 Characteristics of the datasets used in the study

Characteristics/data used	Band	λ (nm)	Acquisition date	Product type	Sensor mode	Platform	Order	Swath (km)	Resolution
Sentinel-1 (VH and VV)	C-band	5546 5760	28/04/2018	SLC	IW	S1A	Descending	250	5 m × 20 m
Sentinel-2	Blue	492.1	27/04/2018 and 30/04/2018	S2MSI1C	MSI Imaging	S2B		290	10 m
	Green	559.0							
	Red	664.9							
	NIR	832.9							

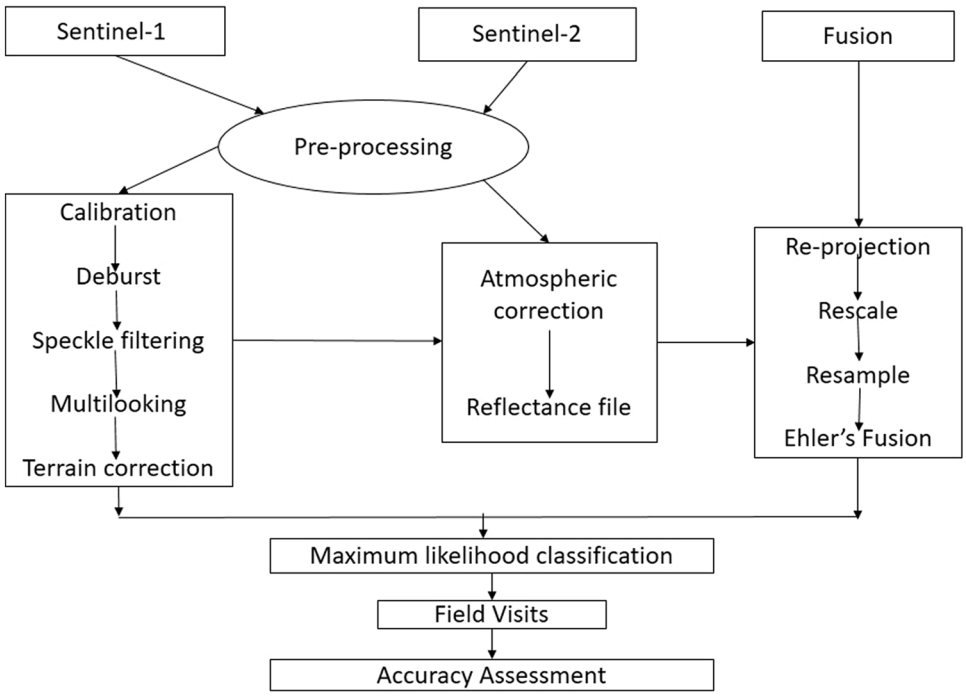

Fig. 2 Flow chart of the methodology adopted in the present study

3.1 Sentinel-1

Three tiles of Level-1, Sentinel-1, Single Look Complex (SLC) data covering the entire area was downloaded from (https://scihub.copernicus.eu/dhus/) official ESA website and pre-processing was initiated using Sentinel Application Platform (SNAP) tool. Sentinel-1 data used in the present study is taken in Interferometric Wide Swath mode at a spatial resolution of (5 m × 20 m) in VV/VH polarization. Pre-processing steps for Sentinel-1 includes calibration, debursting, speckle filtering, multilooking followed by terrain correction. Further, sub-setting is carried out to clip the area of interest because the complete file size is too much large and it becomes difficult to carry out further steps with such huge dataset. After performing the initial pre-processing steps the data is ready to use. Then the conversion from linear to (dB) scale values is performed to obtain negative backscatter values for classification purpose.

Firstly, calibration is carried out to convert intensity images into the Sigma-not (σ_0) images using Sentinel-1 toolbox within SNAP. Unlike other SAR datasets, Sentinel-1 in SNAP does not directly gives the negative backscatter values upon performing the calibration. However, it does give the σ_0 image but the values are in the linear scale. Multilooking of SAR datasets is usually performed to reduce noise and prepare image pixel of perfect square mode. To burst the data of different swaths into single swath seamlessly, terrain observation with progressive scans (TOPS) deburst operation was carried out. Removal of speckle is another key step approaching towards high accuracy classification. Presence of noise affects the radiometric information therefore it is necessary to remove speckle noise, particularly, in case of target identification.

Using single product speckle filter tool, Boxcar filter was applied of 3 × 3 kernel size. In order to eliminate geometric distortions and consequently geo-location errors it is essential to perform terrain correction using range-doppler terrain correction tool. The 1 arc second, 30 m shuttle radar topographic mission (SRTM) data is resampled into 10 m and provide it to range doppler terrain correction for appropriate geo-location information.

3.2 Sentinel-2

Sentinel-2 data acquired from the same source and four adjacent scenes of Sentinel-2 (Level-1C) have been downloaded to cover the entire area. Sentinel-2 consists total 13 bands, spatial resolution of all the bands varies and given in Table 1. Radiometric and atmospheric corrections were applied to generate reflectance file. For Sentinel-2, band 2, 3, 4 and 8 were chosen to prepare RGB in order to obtain better classification accuracy. RGB of the study area is prepared using the boundary shape file to clip the data of the area of interest from all the adjacent scenes. To minimize the difference of different sensing dates and effect of colour and sea m issues, mosaicking was carried out. The RGB of Sentinel-1 and 2 are shown in Fig. 3a, b.

3.3 Field work

The field work were carried out in and around all three districts falls in the study area including Agra, Firozabad and Etawah. Though, the objective was to clearly map the ravine (bad land class occupied area), therefore most of the samples were collected along the main channel in ravenous field. Almost 165 samples were collected initially for different classes and the field photographs taken during ground truth collection are given in Fig. 4. These samples were then arranged for five classes for which the LULC map was prepared and the accuracy assessment was carried out.

3.4 Fusion of Sentinel-1 SAR and Sentinel-2 optical data

Largely, fusion is adopted to overcome the deficiencies of two sensors datasets by merging them into a single output. Single source optical data fusion involves fusion of different bands of two optical sensor images to produce fine resolution image is also termed as spatio-spectral fusion. Blending of optical and SAR datasets to produce enhanced synthetic output vastly acknowledged due to its efficiency for various applications and termed as multisource data fusion. In the presented study, pixel level fusion is adopted which leads to change the pixel values when two data sources gets merged [26]. To carry out fusion analysis for Sentinel-1 SAR and Sentinel-2 optical datasets we have applied Ehlers fusion technique. Different Pan-sharpening methods were comprehensively evaluated by Ehler's including Brovey transformation, principle component analysis or modified Intensity Hue saturation transform and wavelet transformation on different datasets. Basically, fusion is attributed to sharpen the multispectral image with high resolution image without an addition of grey level image [27]. However, SAR data fusion with optical data involves fusion of geometrical and spectral characters along with the spatial characteristics of the datasets. In the present study, rescaling of both the images into unsigned 16 bit scale is carried out. The spatial resolution of Interferometric wide swath mode Sentinel-1 SAR data before processing was (5 × 20) m (range and azimuth) which after processing becomes 12.5 m. Therefore, a nearest neighbour resampling method was applied on Sentinel-1 data to make all the datasets of same spatial resolution i.e., 10 m. In Ehlers fusion, it requires pan sharpened datasets of single band and secondly the multispectral band. One single band is provided as Sentinel-1 (VH polarization) SAR data and second multispectral band will be provided as Sentinel-2 (band 2, 3, 4 and 8) data. In this way a fused image of Sentinel-1 (VH) SAR data and Sentinel-2 is prepared and shown in (Fig. 4c). Similarly, Sentinel-1 (VV) SAR data with Sentinel-2 gets fused and used for the further analysis (Fig. 4d).

4 Results

After pre-processing the datasets, total four images are used including Sentinel-1 SAR (VV, VH and VV + VH) and Sentinel-2 (2, 3, 4 and 8). Two fused images of Sentinel-1 (VH) and Sentinel-2 as well as Sentinel-1 (VV) and Sentinel-2 were also taken into consideration for performing the supervise classification. Supervised classified images of all the datasets including Sentinel-1 (VV, VH and VV + VH), Sentinel-2 and fused datasets are shown in Figs. 5 and 6. The classes in the study area were determined following [28] classification scheme and the obtained areal distribution for all the classes is given in Fig. 7.

4.1 Classification and accuracy assessment of Sentinel-1 and Sentinel-2

Total five classes namely; Water, Urban, Ravines, Barren Land and Cropland, are determined in the study area. Results from Sentinel-1 classification shows the worst scenario when compared with other datasets. Most misclassified pixels found in Sentinel-1 classification are of the water class due to the SAR sensor's high sensitivity towards water and moisture content of the terrain. As far as

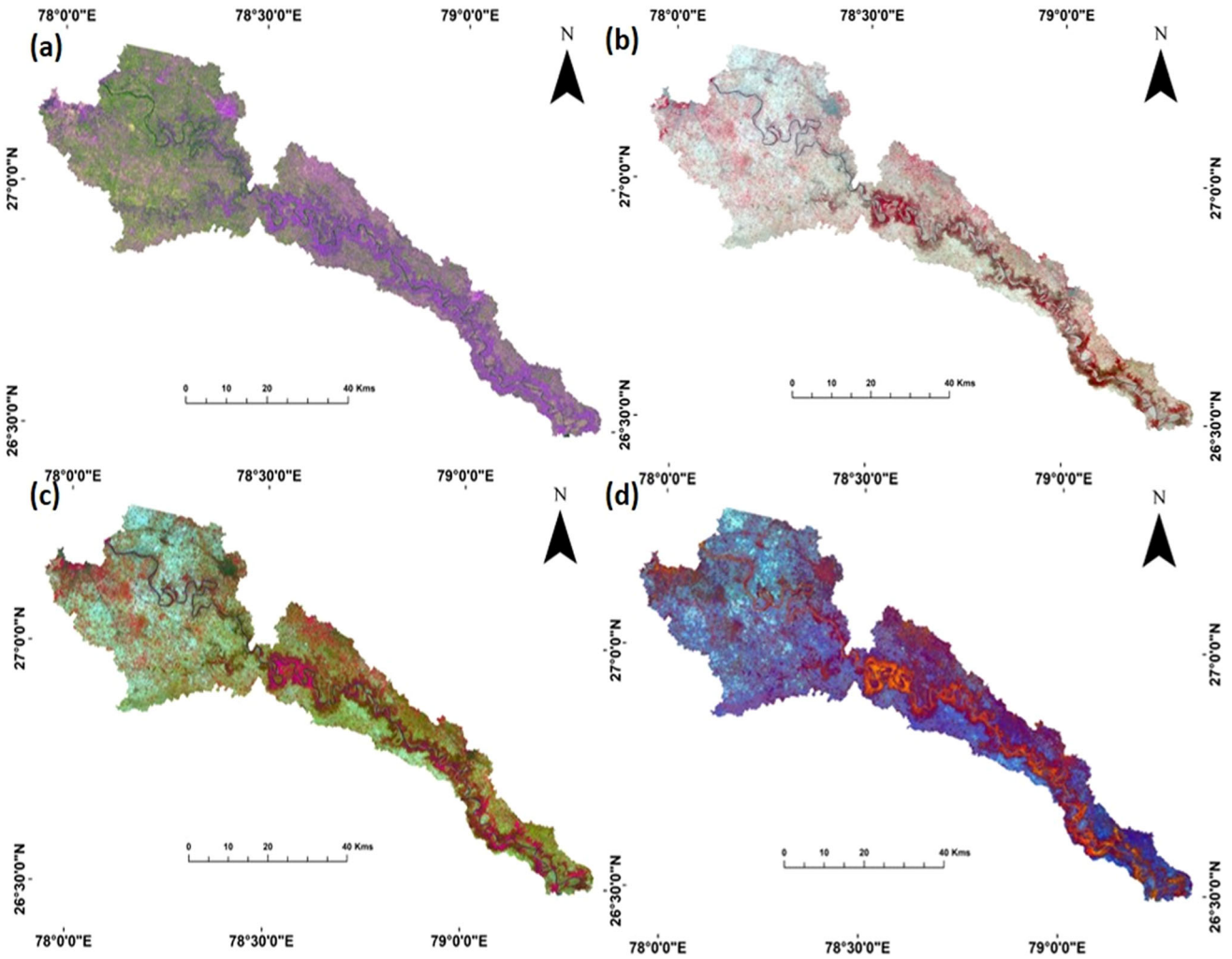

Fig. 3 The prepared datasets for classification, **a** Sentinel-1 RGB of band combination (VH, VV, VV + VH), **b** Sentinel-2 image of band combination (2, 3, 4 and 8), **c** fused image of Sentinel-2 and VH polarization and **d** fused image of Sentinel-2 and VV polarization

the area of different classes are concerned, about 185 km^2 area occupied by water in the area under investigation (Table 2). Water class invades in all the moisture content vulnerable classes, i.e., ravines and settlements. Ravines occupied all the catchment areas along the main channel on both sides and small patches and neighbourhood of settlement pockets along the channel made these classes to be mistakenly predicted. Further, the accuracy assessment is carried out (Table 3) which exhibits users and producers accuracy of each class for all the datasets. It is found that Sentinel-1 having lowest user and producer's accuracy for all the classes especially for water class ascribed to the above mentioned reasons. In addition, the overall accuracy for Sentinel-1 is 60% obtained through Kappa coefficient based confusion matrix (Table 4).

Upon classification the most significant results were obtained for Sentinel-2 datasets. A stacked image of band combination (2, 3, 4, and 8) used for the classification shown in (Fig. 3b). Instead of getting high accuracy in results, Sentinel-2 classified image put urban and water class under category of good saparability. In these images clear cut pattern of two different type of ravines including vegetated and barren ravines can also be recognised. Further, patterns of man- made structures including rail, road and bridges are also clearly visible in the image. Water class in the study area including main Yamuna River channel, canals and ponds occupied an overall area of about 28 km^2 whereas trend of highly urbanized pattern are also traceable by noticing an area of about 180 km^2 occupied by settlement. Moreover, the Ravines and badlands including both vegetated and barren lands spread over an area of 768 km^2 covered 26% area in the present study (Fig. 7). About 100% user and producer accuracy was obtained for water class followed by Ravines and Urban area of about 81 and 80%, respectively. In this way, an overall accuracy of 80% was obtained for the Sentinel-2 optical datasets classified image using maximum likelihood classifier.

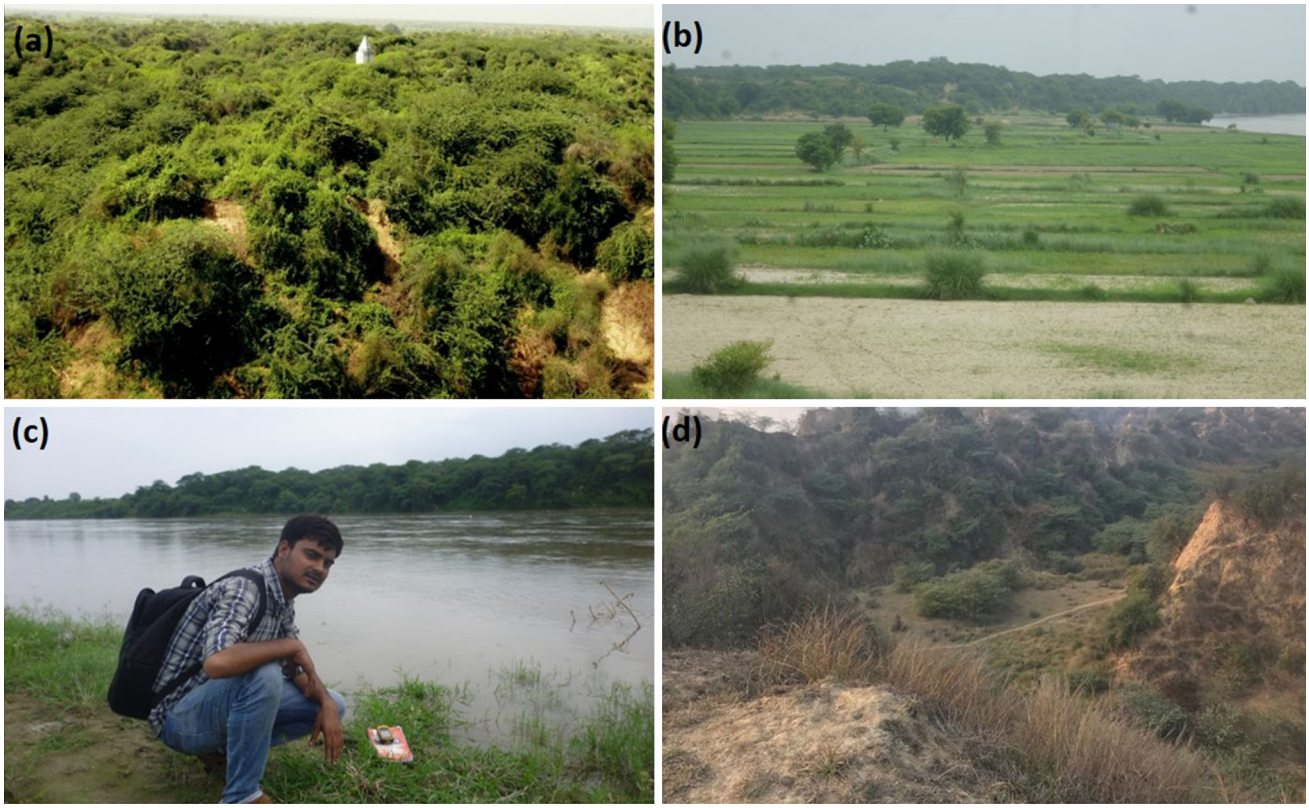

Fig. 4 Field photographs for different classes observed in the field **a** ravenous land spread all across Bah tehsil, Agra district between Yamuna and Chambal, **b** cropland in the vicinity of main channel near Etmadpur tehsil, Agra district. **c** Water class of Yamuna River around Agra city, **d** Barren land class near Firozabad

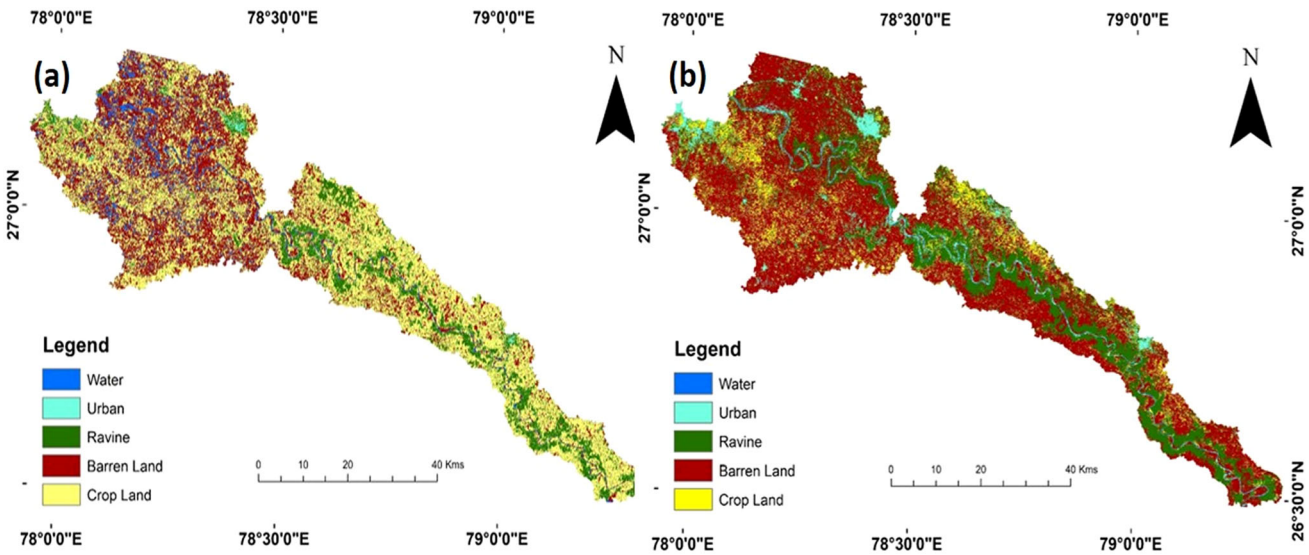

Fig. 5 LULC map prepared for **a** Sentinel-1 and for **b** Sentinel-2 datasets

4.2 Classification and accuracy assessment of synergistic datasets

The fused datasets of different polarization of Sentinel-1 including VV and VH with Sentinel-2 optical datasets using Ehlers fusion technique were assessed by performing LULC classification. It has been observed that a very slight difference in accuracy on Maximum Likelihood algorithm based classification for both the datasets as well their visual interpretation were obtained (Fig. 5). However, as far as

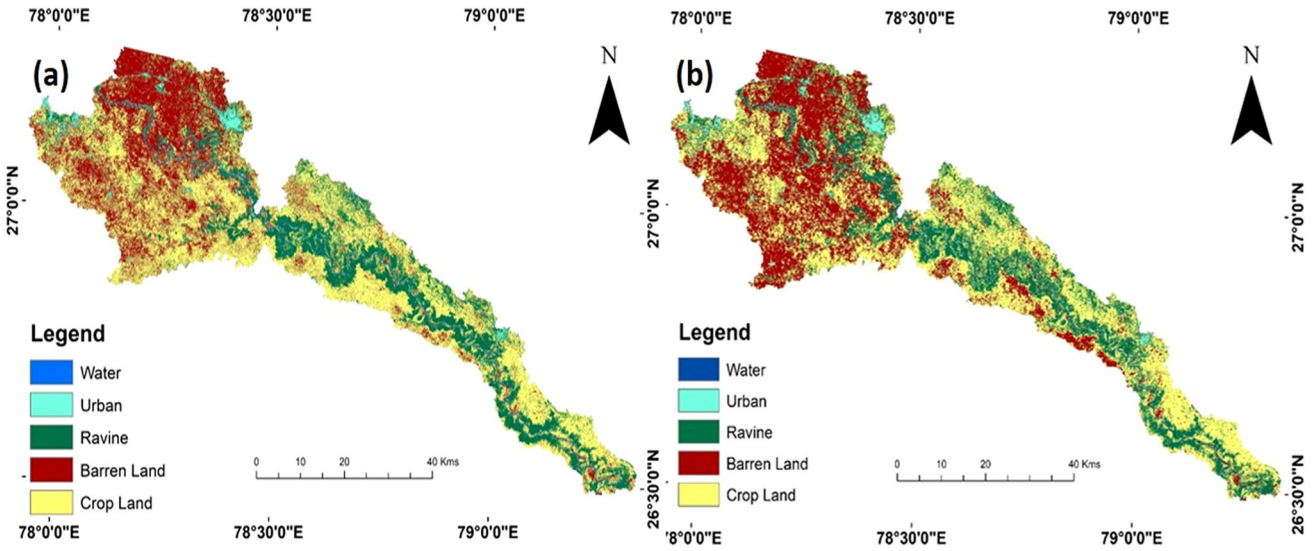

Fig. 6 LULC map prepared for **a** VH-polarization and Sentinel-2 fused image and for **b** VV-polarization and Sentinel-2 fused datasets

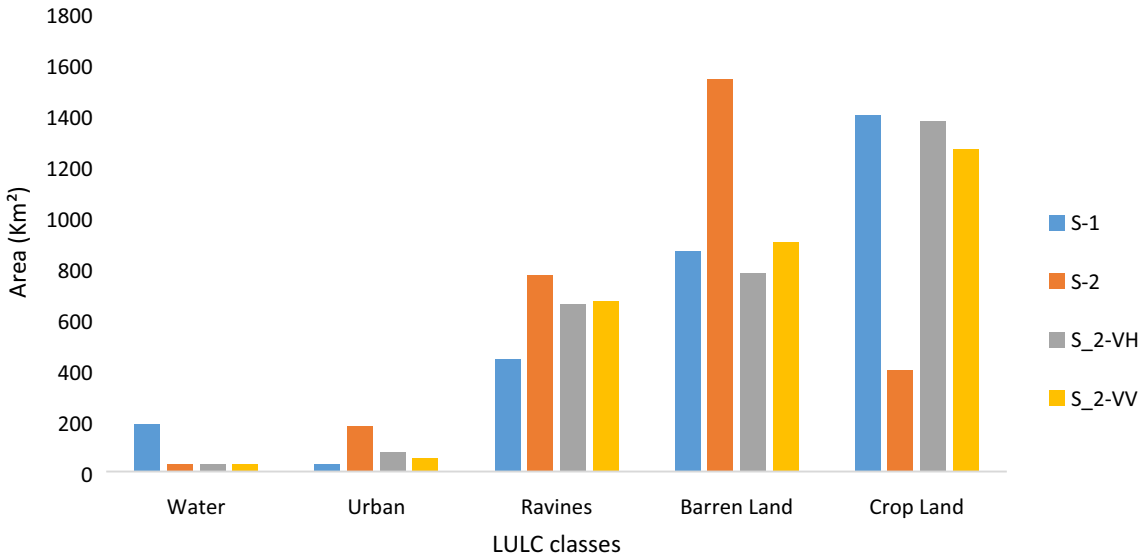

Fig. 7 Area wise distribution of different LULC classes observed in the study area. (*Note* S-1—Sentinel-1, S-2—Sentinel-2, S-2–VH—Sentinel-2 and VH fused datasets and S-2–VV—Sentinel-2 and VV fused datasets)

Table 2 Area wise distribution of different classes obtained in classification of different datasets

Datasets/classes	Sentinel-1		Sentinel-2		Fused (VH-S-2)		Fused (VV-S-2)	
	Area	Area%	Area	Area%	Area	Area%	Area	Area%
Water	186.64	6.40196	28.076	0.96305	28.403	0.97426	29.7368	1.01999
Urban	27.979	0.95971	180.02	6.17497	78.137	2.68016	52.2776	1.79315
Ravines	440.72	15.1171	768.66	26.3657	657.18	22.5417	669.764	22.9733
Barren Land	862.44	29.5822	1539.8	52.8188	778.79	26.7131	899.534	30.8545
Crop Land	1397.62	47.93893	398.748	13.67731	1372.89	47.09068	1264.086	43.35892

the VH-polarization is concerned it gives an overall accuracy of 85% which is found to be the highest in the present study. Water class in VH-polarized fused image is clearly separable whereas barren and crop land are mistakenly predicted. The most striking observation is for Ravine and Urban class mapping where both user and producer

Table 3 User and producer accuracy obtained for different classes in classification of different datasets

Datasets/classes	Sentinel-1		Sentinel-2		Fused (VH-S-2)		Fused (VV-S-2)	
	UA (%)	PA (%)	UA (%)	PA (%)	UA (%)	PA (%)	UA (%)	PA (%)
Water	32	100	100	100	100.0	100.0	100.0	100.0
Urban	56	93.33	64	80	80.00	95.24	80.00	90.91
Ravines	72	51.43	72	81.82	80.00	95.24	76.00	73.08
Barren	72	81.82	88	68.75	80.00	74.07	80.00	86.96
Crop	68	37.78	76	73.08	88.00	70.97	84.00	72.41

Table 4 Kappa coefficient and overall accuracy for all the classified datasets

Datasets	Overall accuracy (%)	Kappa coefficient
Sentinel-1	60.00	0.5
Sentinel-2	80.00	0.75
Fused (VH-S-2)	85.60	0.82
Fused (VV-S-2)	84.00	0.8

accuracy are very high. VV-polarized fused image also followed the similar trends. Separate classified image windows for urban and ravine classes are prepared which exhibits clear cut demarcation of these two classes (Fig. 8). This window also gives a good visualization for all misclassified as well as well classified features in the image. Area wise distribution shows that 28% area is occupied by water which is similar as obtained for Sentinel-2 while VV-polarized fused image also shows a similar trend for water class with a slight deviation. Further, the area occupied by ravines, more or less, similarly predicted by Sentinel-2, Fused (VH-S-2) and by Fused (VV-S-2). Moreover, an overall accuracy for VV-polarized fused image with Sentinel-2 is 84%.

4.3 Kappa coefficient

Accuracy assessment of all the classified image were performed using Kappa coefficient based confusion matrix. Kappa coefficient values ranges from -1 to $+1$ which gives an idea about the reliability of the test [29]. The value 1 stands for more or less most reliable results whereas the values towards -1 shows decline in the reliability. In the present study the Kappa Coefficient for Sentinel-1 and Sentinel-2 are 0.5 and 0.75, respectively, indicates that the Sentinel-2 image is classified more accurately. Similarly the Fused images of VH and VV polarization with Sentinel-2 data shows (K) values of 0.82 and 0.8 respectively (Table 4). Overall, the Kappa values further validates that VH-polarized image with Sentinel-2 has given the best results in the present study.

5 Discussion

In the presented study, the area is highly suffered region from the problem of ravenous erosion (formation of badlands) which subsequently causes nutrient deficiency, moisture stress and biotic interference in the region. About 7.5 lac ha area in Uttar Pradesh is occupied by Ravines as per the National Remote Sensing Centre report 2005. High uneconomic farming in the region where agriculture is the dominant occupation of the people requires to deal this problem on priority level. Further, this highly undulated region is also pose a threat to socio-economic fabric of the region by being served as the shelter for Dacoits. These wasteland in the study area causes physical, chemical and vegetal degradation of land. Several type of erosional processes, waterlogging problem, lowering of water table, salt affected soil, declining fertility, deforestation and overgrazing are the main issues associated with these wasteland [30]. Several National as well as International agencies including World Bank and European Union recognise the problem and has launched several schemes for reclamation. Therefore, a proper understanding about the extent, nature and associate land cover features is a prerequisite for the sustainable development of these degraded lands. However, mapping with optical datasets carried out by several workers but SAR datasets found complementary to the optical sensing still remains unexplored for these wasteland mapping practices.

The aim of the presented study is to evaluate different datasets for high accuracy LULC mapping in the study area. The MLC classified maps of the Sentinel-1 and Sentinel-2 and their combinations are presented in the (Figs. 5, 6) as the best accurate results obtained using freely available optical and SAR imageries. The application of fusion technique encompasses a broad spectrum. It enables to separate the objects on the basis of all the characteristic including spectral signature, dielectric properties and the surface roughness of the objects [31]. In the fusion, nearest neighbour resampling was applied on Sentinel-1 VH image to improve and match the spatial resolution of the image with Sentinel-2 image. The classification of Sentinel-1 (a combination of VH, VV and VH/VV) of 10 m spatial resolution suggests that

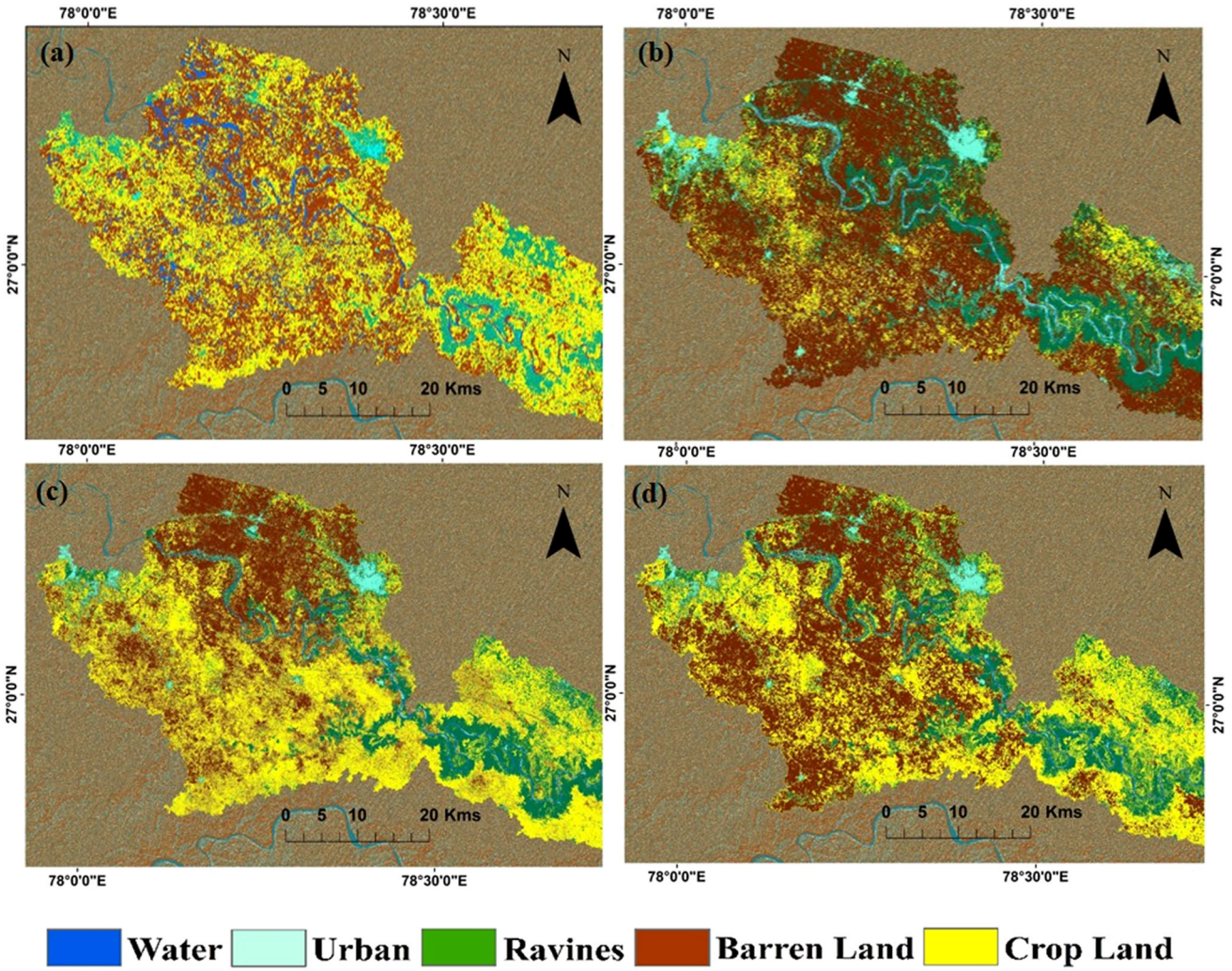

Fig. 8 Comparison of LULC classes obtained on different datasets **a** Sentinel-1 classified image, **b** Sentinel-2, **c** VH and Sentinel-2 fused datasets classified image and **d** VV and Sentinel-2 fused datasets classified image

resampling or increased spatial resolution does not affects the classification accuracy, however, it enhance the data size. This is also obvious in the results, showing that the overall accuracy is higher in case of fused data of Sentinel-1, VH polarization and Sentinel-2 data. An overall increase in accuracy for fused datasets in comparison to optical data ranges from $\pm$ 4 to $\pm$ 5. Except for Sentinel-1 datasets, the user and producer accuracy found good for all the classes (Fig. 9). This improvement is further obvious in users and producers accuracy, particularly for ravines or badlands class. In this way, the results obtained are in consistency with the previous work on fusion techniques of SAR and optical datasets [9]. Visual inspection of the images also suggested that the fused datasets provided the best classification and corresponds to existing land covers much closely (Fig. 6). All the areas near the main channel and towards eastern portion of the study area are highly covered with these badlands also falls in the badlands category in the classified results.

However, the data for the present study were acquired for the April month, due to unavailability of water in the region. During monsoon period, all the erosional landforms or badlands gets flooded with water, therefore, suitable LULC mapping and estimation of these badlands occupied area becomes irrelevant. Most of the land covers particularly the settlements are the temporary shelters in the region, however, increasing existing trends of urbanization cannot be ruled out. In the presented study, all the datasets shows an almost similar trend for the area occupied by ravine class except Sentinel-1 probably due to its high sensitivity towards moisture. The area along the main channel contains muddy to little bit wetted nature of land was classified as water class in Sentinel-1 classification. However, it shows an area of about 15% to the total study area, occupied by ravine class. The most accurate

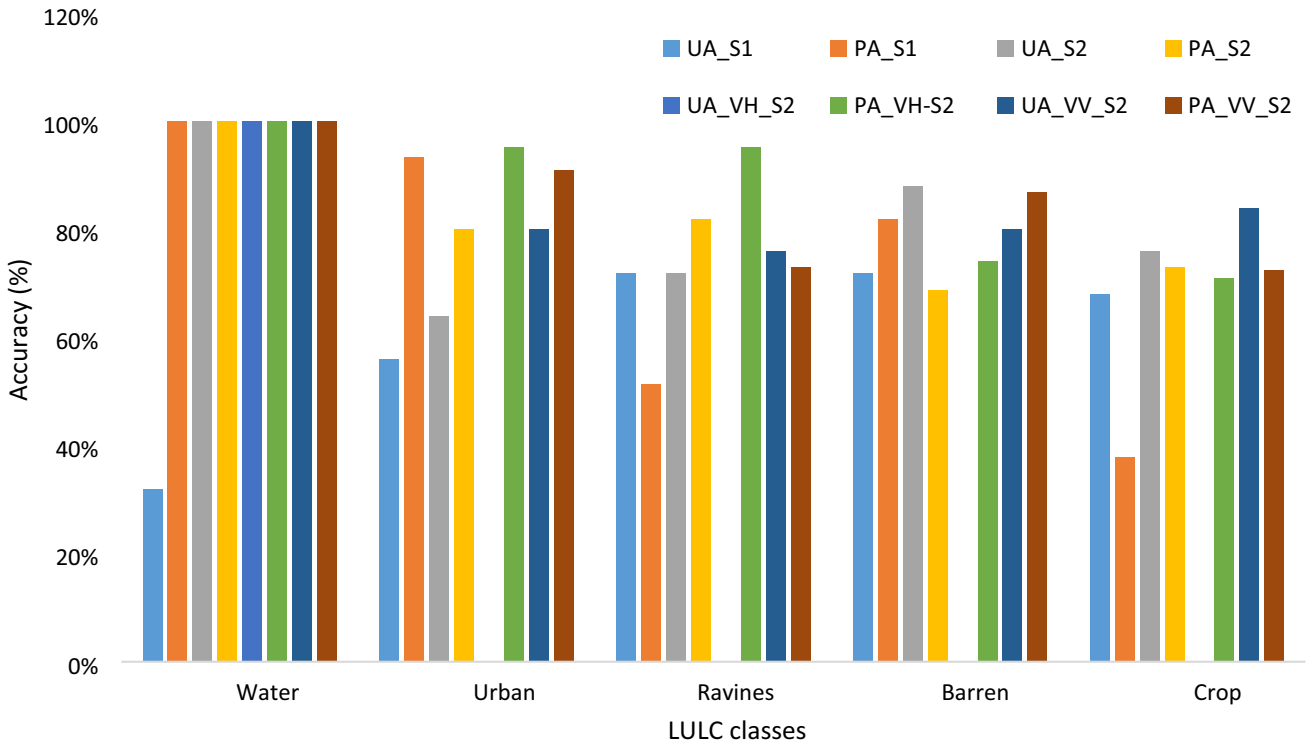

Fig. 9 Accuracy of different classes obtained for different datasets. (*Note* UA_S1—User accuracy for Sentinel-1, PA_S2—Producer accuracy for Sentinel-2, UA_VV_S2—User accuracy for VV and Sentinel-2 fused dataset, PA_S1—producer accuracy for Sentinel-1, UA_VH_S2—user accuracy for VH and Sentinel fused datasets, PA_VV_S2—producer accuracy for VV and Sentinel-2 fused dataset, UA_S2—user accuracy for Sentinel-2, PA_VH_S2—producer accuracy for VH and Sentnel-2 fused datasets)

estimation of ravine class (wasteland) is shown by fused combination of Sentinel-1 (VH) and Sentinel-2, shows an overall area of about 657 km^2 (22%) out of 2915 km^2. Therefore, the single SAR data has given most misclassified results and found erratic in terms of LULC mapping. This is probably occurred due to presence of high moisture content land available in and around the main river channel.

The study proposed integration of optical and SAR datasets based methodology for high accuracy LULC classification particularly for ravine mapping in the study area. Previous work carried out using fusion technique for optical and SAR datasets suggested a high accuracy LULC mapping can be achieved using these datasets. Soria-Ruiz et al. [31] highlighted the fusion technique for Radarsat-1 and Landsat-7 for urban growth and vegetation mapping and numerous similar studies were also carried out for SAR and optical data fusion for high accuracy mapping. There are numerous classification algorithm and ML may not provide best accurate results but other advanced classification algorithms with Full and hybrid polarimetric datasets could have provided much more specified observations. Classification algorithm such as random forest, support vector machine, artificial neural network and decision tree classifiers were suggested in different studies to improve the accuracy of SAR and fused datasets classification. However, several attempts were made by different workers to clearly demarcate the boundary of these badlands in order to understand the expansion dynamics of these ravines. Thus, high accuracy LULC maps are indispensable of the study area.

Still, the SAR polarimetry has given the prominent results in the classification of different features on the land [10]. But, the presented investigation focused on the classification of bad land areas in and around the Yamuna River main channel with freely available dual polarimetric SAR and optical datasets. Therefore, adding the freely available SAR datasets to optical data can be considered to improve the classification for addressing the land degradation problems. In the study, we have focused on dual polarized freely available SAR data and basic polarimetric techniques involving band math for classification purpose. Although, selections of high resolution bands, suitable fusion method, visual inspection and comprehensive analysis of all the features are the pre requisite to prepare high accuracy maps. Moreover, rainy days should be avoided for image acquisition in order to improve the accuracy of LULC maps because in rainy season entire badland areas gets inundated with water. Therefore actual demarcation of badland occupied area become ambiguous. However, in the

present study C-band Sentinel-1 data appears to provide satisfactory results but the L-band SAR datasets has the capability to explore much more details including morphology and shape of these undulated terrains. Finally, the study suggested that fusion technique provided most reliable results, however, several other classification algorithms and datasets with available polarimetric techniques can also be explored for detailed classification of the intensity of degradation in these waste lands.

6 Conclusion

The aim of the study was the accuracy assessment of fused, optical and SAR datasets for LULC mapping with special reference to badlands class in the study area. A successful demonstration of Sentinel-1 and Sentinel-2 performance for LULC mapping in the study area is also provided. The application of Ehlers fusion technique is assessed on different polarization (VV and VH) fused datasets by obtaining highly precise results and found that fusion is significantly improved the accuracy of classification. Cross polarized VH, SAR data with Sentinel-2 data has given the most accurate results, however, the performance of Sentinel-2 is also noticeable. The poor performance of Sentinel-1 is attributed to its high sensitivity towards soil moisture, therefore, shown highly intermixed classes of moist ravines into the water class. This is the first attempt in the study area using up to date space technology for high accuracy LULC map preparation in the study area useful in land degradation monitoring and assessment studies. Moreover, reclamation of these ravines using new approaches is under progress but the maximum utilization of newly available space technology to strengthen the rehabilitation processes in these highly populated region is also recommended.

Compliance with ethical standards

Conflict of interest On behalf of all the authors, I confirmed that there is no conflict of interest.

References

1. Chatterjee, R. S., Saha, S. K., Kumar, S., Mathew, S., Lakhera, R. C., Dadhwal, V. K., et al. (2009). Interferometric SAR for characterization of ravines as a function of their density, depth, and surface cover. *ISPRS Journal of Photogrammetry and Remote Sensing, 64*(5), 472–481.
2. Marzolff, I., & Pani, P. (2018). Dynamics and patterns of land levelling for agricultural reclamation of erosional badlands in Chambal Valley (Madhya Pradesh, India). *Earth Surface Processes and Landforms, 43*(2), 524–542.
3. Zinck, J. A., Lopez, J., Metternicht, G. I., Shresthaa, D. P., Vázquez-Selem, L. L., et al. (2001). Mapping and modelling mass movements and gullies in mountainous areas using remote sensing and GIS techniques. *International Journal of Applied Earth Observation and Geoinformation, 3*(1), 43–53.
4. Kala, S., Meena, H. R., Rashmi, I., Prabavathi, M., Singh, A. K., Singh, R. K., et al. (2017). Status of medicinal plants diversity and distribution at rehabilitated Yamuna and Chambal ravine land ecosystems in India. *International Journal of Current Microbiology and Applied Sciences, 6*(3), 618–630.
5. Mohapatra, S. N., Rompaey, A. V., Pani, P., Poesen, J., Ranga, V., et al. (2016). Detection and analysis of badlands dynamics in the Chambal River Valley (India), during the last 40 (1971–2010) years. *Environmental Earth Sciences, 75*(3), 183.
6. Bali, J. S., Kamphrost, A., Miejerink, A. M. J., & Hilwig, F. W. (1969). *Methods and the legend for the use of aerial photographs in the survey, stabilization and reclamation of ravines*. New Delhi: Central Ravine Reclamation Board, Ministry of Agriculture and Co-operation.
7. Reiche, J., Verbesselt, J., Hoekman, D., Herold, M., et al. (2015). Fusing Landsat and SAR time series to detect deforestation in the tropics. *Remote Sensing of Environment, 156,* 276–293.
8. Haas, J., & Ban, Y. (2017). Sentinel-1A SAR and Sentinel-2A MSI data fusion for urban ecosystem service mapping. *Remote Sensing Applications: Society and Environment, 8*(1), 41–53.
9. Steinhausen, M. J., Wagner, P. D., Narasimhan, B., Waske, B., et al. (2018). Combining Sentinel-1 and Sentinel-2 data for improved land use and land cover mapping of monsoon regions. *International Journal of Applied Earth Observation and Geoinformation, 73*(April), 595–604.
10. Tavares, P. A., Beltrão, N. E. S., Guimarães, U. S., Teodoro, A. C., et al. (2019). Integration of Sentinel-1 and Sentinel-2 for classification and LULC mapping in the urban area of Belém, eastern Brazilian Amazon. *Sensors, 19*(5), 1140.
11. Khan, A., Rao, L. A. K., Yunus, A. P., & Govil, H. (2018). Characterization of channel planform features and sinuosity indices in parts of Yamuna River flood plain using remote sensing and GIS techniques. *Arabian Journal of Geosciences, 11*(17), 525.
12. Ali, P. Y., Jie, D., Khan, A., Sravanthi, N., Rao, L. A. K., Hao, C., et al. (2019). Channel migration characteristics of the Yamuna River from 1954 to 2015 in the vicinity of Agra, India: A case study using remote sensing and GIS. *International Journal of River Basin Management, 17*(3), 1–9.
13. Kaplan, G., & Avdan, U. (2018). Sentinel-1 and Sentinel-2 data fusion for wetlands mapping: Balikdami, Turkey. *International Archives of the Photogrammetry, Remote Sensing and Spatial Information Sciences—ISPRS Archives, 42*(3), 729–734.
14. Ban, Y., Webber, L., Gamba, P., & Paganini, M., et al. (2017). EO4Urban: Sentinel-1A SAR and Sentinel-2A MSI data for global urban services. In *2017 Joint urban remote sensing event (JURSE)* (Vol. 1, No. 3, pp. 1–3).
15. Hong, G., Zhang, A., Zhou, F., Brisco, B., et al. (2014). Integration of optical and synthetic aperture radar (SAR) images to differentiate grassland and alfalfa in Prairie area. *International Journal of Applied Earth Observation and Geoinformation, 28*(1), 12–19.
16. Amarsaikhana, D., Blotevogel, H. H., Van-Genderenc, J. L., Ganzorig, M., Gantuya, R., & Nergui, B. (2010). Fusing high-resolution SAR and optical imagery for improved urban land cover study and classification. *International Journal of Image and Data Fusion, 1*(1), 83–97.
17. Clerici, N., Calderón, C. A. V., Posada, J. M., et al. (2017). Fusion of Sentinel-1a and Sentinel-2A data for land cover mapping: A case study in the lower Magdalena region, Colombia. *Journal of Maps, 13*(2), 718–726.
18. Malenovský, Z., Rott, H., Cihlar, J., Schaepman, M. E., Santos, G. G., Fernandes, R., et al. (2012). Sentinels for science: Potential

of Sentinel-1, -2, and -3 missions for scientific observations of ocean, cryosphere, and land. *Remote Sensing and Environment, 120,* 91–101.
19. Sprohnle, K., Fuchs, E. M., & Pelizari, P. A. (2017). Object-based analysis and fusion of optical and SAR satellite data for dwelling detection in refugee camps. *IEEE Journal of Selected Topics in Applied Earth Observations and Remote Sensing, 10*(5), 1780–1791.
20. Gibril, M. B. A., Bakar, S. A., Yao, K., Idrees, M. O., & Pradhan, B. (2017). Fusion of RADARSAT-2 and multispectral optical remote sensing data for LULC extraction in a tropical agricultural area. *Geocarto International, 32*(7), 735–748.
21. Sanli, F. B., Abdikan, S., Esetlili, M. T., & Sunar, F. (2017). Evaluation of image fusion methods using PALSAR, RADARSAT-1 and SPOT images for land use/land cover classification. *Journal of the Indian Society of Remote Sensing, 45*(4), 591–601.
22. Klonus, S., & Ehlers, M. (2008). Image fusion using the Ehlers spectral characteristics preservation algorithm. *GIScience & Remote Sensing, 44*(2), 93–116.
23. Ehlers, M. (2004). Spectral characteristics preserving image fusion based on Fourier domain filtering. In *Remote sensing for environment monitoring, GIS applications and geology IV* (Vol. 5574, No. 1).
24. Dimov, D., Kuhn, J., Conrad, C., et al. (2016). Assessment of cropping system diversity in the Fergana valley through image fusion of Landsat 8 and Sentinel-1. *ISPRS Annals of the Photogrammetry, Remote Sensing and Spatial Information Sciences, 3*(July), 173–180.
25. Kottek, M., Grieser, J., Beck, C., Rudolf, B., Rubel, F., et al. (2006). World map of the Köppen–Geiger climate classification updated. *Meteorologische Zeitschrift, 15*(3), 259–263.
26. Pal, S. K., Majumdar, T. J., & Bhattacharya, A. K. (2007). ERS-2 SAR and IRS-1C LISS III data fusion: A PCA approach to improve remote sensing based geological interpretation. *ISPRS Journal of Photogrammetry and Remote Sensing, 61*(5), 281–297.
27. Ehlers, M., Klonus, S., Åstrand, P. J., & Rosso, P. (2010). Multi-sensor image fusion for pansharpening in remote sensing. *International Journal of Image and Data Fusion, 1*(1), 25–45.
28. Anderson, J. R. (1976). *A land use and land cover classification system for use with remote sensor data* (Vol. 964). Washington, DC: US Government Printing Office.
29. Grouven, U., Bender, R., Ziegler, A., & Lange, S. (2007). The kappa coefficient. *Deutsche Medizinische Wochenschrift, 132*(Suppl), 1–4.
30. Reddy, G. P. O., Kumar, N., & Singh, S. K. (2018). Remote sensing and GIS in mapping and monitoring of land degradation. *Geospatial Technologies in Land Resources Mapping, Monitoring and Management, 21,* 401–424.
31. Soria-Ruiz, J., Fernandez-Ordoñez, Y., & Woodhouse, I. H. (2010). Land-cover classification using radar and optical images: a case study in Central Mexico. *International Journal of Remote Sensing, 31*(12), 3291–3305.